Spectrum of Engineering Sciences
ISSN (e) 3007-3138 (p) 3007-312X Volume 4, Issue 4, 2026

GREEN SYNTHESIS OF SILVER NANOPARTICLES USING PLANT EXTRACTS FOR ENHANCED ANTIMICROBIAL AND WOUND HEALING APPLICATIONS

Javeria Mehmood[1], Aijaz Ahmed Bhutto[2], Zain-ul-Abideen[*3]

[1]*Department of Chemistry Emerson University Multan Pakistan*
[2]*Dr. M.A Kazi Institute of Chemistry, University of Sindh, Jamshoro 76080, Pakistan*
[*3]*Institute of Chemical Sciences Bahaudin Zakariya University Multan, Pakistan*

[1]javeriamehmood1007@gmail.com, [2]bhutto.aijaz@usindh.edu.pk, [*3]zk6442278@gmail.com

DOI: https://doi.org/10.5281/zenodo.19564772

Keywords
Green synthesis, silver nanoparticles (AgNPs), Plant extract, antimicrobial activity, Antioxidant activity, Wound healing, Cytotoxicity, Nanobiotechnology, Biomedical applications

Article History
Received: 16 February 2026
Accepted: 26 March 2026
Published: 14 April 2026

Corresponding Author: *
Zain-Ul-Abideen

Abstract

Silver nanoparticles (AgNPs) have emerged as promising nanomaterials in biomedical applications due to their strong antimicrobial and wound healing properties. This study focuses on the eco-friendly green synthesis of AgNPs using plant extracts as natural reducing and stabilizing agents, addressing the limitations of conventional chemical synthesis methods that involve toxic reagents and environmental hazards. The methodology involved preparation of plant extract followed by its reaction with silver nitrate under controlled conditions to synthesize AgNPs. The nanoparticles were purified and characterized using advanced analytical techniques including UV–Visible spectroscopy, FTIR, XRD, SEM, and EDX to determine their optical, structural, and morphological properties. The results confirmed successful synthesis of crystalline, nanoscale AgNPs with a characteristic surface plasmon resonance peak at 404 nm. Biological evaluations demonstrated significant antimicrobial activity against Staphylococcus aureus, Escherichia coli, and Candida albicans, with a concentration-dependent increase in inhibition zones and low minimum inhibitory concentration (MIC) values. The nanoparticles also exhibited considerable antioxidant activity, achieving up to 78.6% radical scavenging efficiency. Cytotoxicity analysis revealed good biocompatibility, maintaining over 80% cell viability at concentrations ≤50 µg/mL. Furthermore, in vitro scratch assay results showed enhanced fibroblast migration and accelerated wound closure, reaching approximately 87.9% healing within 24 hours.

In conclusion, plant-mediated AgNPs demonstrate multifunctional properties including antimicrobial, antioxidant, and wound healing capabilities. The study highlights their potential as sustainable and effective alternatives for biomedical applications, particularly in wound management, while emphasizing the need for further in vivo investigations for clinical translation.

Graphical Abstract

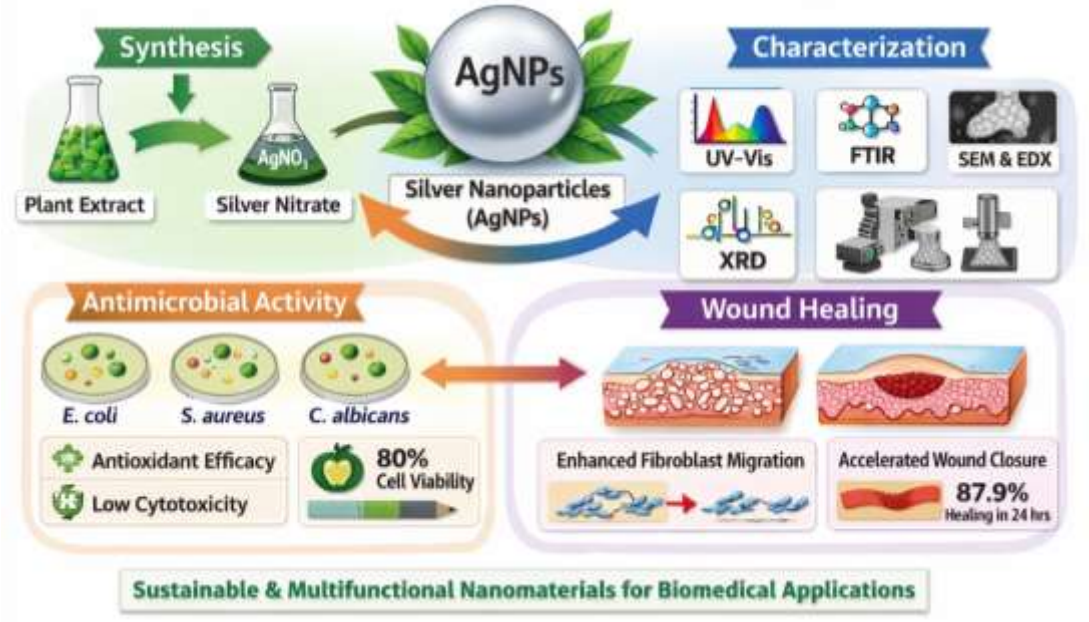

1 INTRODUCTION

AgNPs are one of the most widely researched nanomaterials in biomedical science because of their special physicochemical features such as the high surface-to-volume ratio, adjustable optical behavior and excellent antimicrobial action (Palanisamy et al., 2025). AgNPs have been extensively studied in the last twenty years in diverse applications including drug delivery and biosensing, antimicrobial surfaces and wound care. Their antimicrobial effect has wide spectrum against Gram-positive and Gram-negative microbes and fungi, making them promising antimicrobial agents in the face of increased resistance to antimicrobial agents (Nandhini et al., 2023). Concurrently, the growing need of safe, affordable and sustainable synthesis pathways has led to a surge of focus on the green methods of nanotechnology. Traditional approaches towards the synthesis of silver nanoparticles like chemical reduction, thermal decomposition and electrochemical processes typically entail the use of dangerous chemicals, intense energy sources and elaborate processes that may produce toxic by-products (Aldakheel, Sayed, Mohsen, Fagir, & El Dein, 2023). Such limitations do not only raise concerns of environmental and safety but limit their biomedical use, as it has the potential to cause cytotoxic effects. Alternatively, biological-based green synthesis systems (plant extracts, microorganisms, biomolecules) have become of significant interest as environmentally friendly and sustainable alternatives (Qubtia et al., 2024). Among them, the plant-mediated synthesis is unique due to its simplicity, speed, scalability, and the high diversity of bioactive compounds found in the plant systems.

The number of phytochemicals in plant extract is very large and can include flavonoids, phenolic acids, terpenoids, alkaloids, and proteins, all of which can be simultaneously reducing and stabilizing agents in nanoparticle production (Lakkim et al., 2023). These biomolecules help transform silver ions (Ag ions) to metallic silver (Ag 0) as well as cap the nanoparticles so as to avoid aggregation and improve stability. This two-fold functionality removes the usage of extra chemical reagents and thus the process is not only cost-effective but also ecologically harmless. Moreover, the size, morphology and biological performance of the synthesized nanoparticles can greatly depend on the nature and composition of phytochemicals, thus providing the possibility to optimize the properties of nanoparticles to a given use (Osman Mahmud et al., 2025). Plant-mediated AgNPs have a biomedical interest especially in

infectious disease and wound healing. Microbial infections complicate chronic wound, such as diabetic ulcers, burns, and surgical wounds, and slow the healing period, making severe complications more likely (Assad et al., 2025). This has been further complicated by the emergence of multidrug-resistant (MDR) pathogens, which have necessitated the need to come up with alternative antimicrobial plans. Silver nanoparticles have been shown to interrupt the cell membranes of microbes, produce reactive oxygen species (ROS) and disrupt DNA replication, which result in effective microbial inhibition. These nanoparticles can have improved biological activity when they are synthesized with plant extracts because of the synergistic effects of residual phytochemicals on the surface of the nanoparticles. Besides antimicrobial effects, AgNPs have demonstrated promising potential in the promotion of wound healing in several ways (Ahmad et al., 2023). They are the modulation of the inflammatory responses, stimulation of fibroblastic proliferation, promotion of collagen deposition, and epithelialization (Bharali et al., 2023). These effects can be further enhanced by the addition of plant-derived compounds, which can add antioxidant and anti-inflammatory properties essential to effective tissue repair. Antioxidants are important in countering the excessive free radicals in the wound site, which decreases the oxidative stress at the wound site, thus increasing the healing process. As a result, the green-synthesized AgNPs are a versatile platform integrating antimicrobial, antioxidant, and regenerative functions (A. R. Sharma, Sharma, Nath, & Lee, 2024). Although the green synthesis of silver nanoparticles has drawn increasing literature, there are still a number of challenges and research gaps. A great deal of research is concentrated on synthesis and general characterization, with little ability to provide mechanistic understanding and thorough biological analyses. In addition, plant extract composition and synthesis conditions, and characterization methods may vary, introducing inconsistencies in nanoparticle properties and biological behavior (S. Sharma, Bose, Biswas, Sen, & Roy, 2025). It is also necessary that systematic studies be done that can correlate physicochemical properties with biological processes especially in wound healing. These gaps need to be addressed to promote the clinical translation of nanomaterials green-synthesized (Gangwar et al., 2025). Against this backdrop, the current research project will formulate a simple and green technique of silver nanoparticles through plant extracts and their suitability in antimicrobial and wound healing uses. The synthesized nanoparticles are systematically analyzed by the application of sophisticated analytical methods to ascertain their structural, morphological and chemical attributes (Iqbal et al., 2024). Moreover, their biological efficacy is determined by antimicrobial testing against specific pathogenic microorganisms, antioxidant testing, cytotoxicity testing as well as in vitro wound healing systems (Franceschinis et al., 2023). Through green synthesis and thorough characterization and biological assessment, this research aims to make a contribution towards the creation of sustainable nanomaterials that have greater therapeutic prospects in biomedical applications (Abdel-Wahab et al., 2024).

2 Materials and Methods

These chemicals used were of analytical grade and there was no further purification needed before using them. These chemicals are Silver nitrate ($AgNO_3$, ≥99% purity), Distilled water / Deionized water, Ethanol (analytical grade), Methanol (analytical grade), Nutrient agar (NA), 2,2-Diphenyl-1-picrylhydrazyl (DPPH) (sigma Aldrich), Ascorbic acid (standard antioxidant), Dulbecco's Modified Eagle Medium (DMEM), Fetal bovine serum (FBS), Penicillin–streptomycin solution, Trypsin–EDTA solution, Phosphate-buffered saline (PBS), MTT reagent (3-(4,5-dimethylthiazol-2-yl)-2,5-diphenyl tetrazolium bromide), Dimethyl sulfoxide (DMSO).

2.1 Instrument

Magnetic stirrer with hot plate, pH meter, Centrifuge (high-speed), Hot air oven, Analytical balance, Micropipettes (various ranges), Water bath, Refrigerator (4°C), Deep freezer (−20°C or −80°C), Incubator (37°C), Autoclave.

2.2 Preparation of Plant Extract

New plant material (leaf/root/flowers, depending on the chosen species) was gathered in a local source and confirmed by a professional botanist. The plant material was carefully washed with the help of a running tap water to remove dust and impurities, and then washed with distilled water to remove the rest of the contaminants. The samples were subsequently air-dried at room temperature (7-10 days) to dry the samples and retain the bioactive compounds and prevent thermal degradation of the samples. The plant material was dried completely and then ground in a mechanical grinder into a fine powder and stored in airtight containers until further use. To extract, a sample of the dried plant powder (1020 g), was added to the solvent (100200 mL of distilled water or ethanol, as suitable to the method of extraction) with a known amount of the known powder, and the mixture was heated at 60-80°C and stirred with constant motion. The blend was left to cool down to room temperature and filtered with Whatman No. 1 filter paper to eliminate the particulates. The plant extract was then collected as a resultant filtrate which was stored at 4°C to be used later in the synthesis of silver nanoparticles under green conditions (Patel, Singh, & Singh, 2023).

2.3 Green Synthesis of Silver Nanoparticles (AgNPs)

Synthesis of silver nanoparticles was done greenly by using the prepared plant extract as a reducing as well as stabilizing agent. A solution containing 1 mM silver nitrate ($AgNO_3$) was made by dissolving 0.017 g of $AgNO_3$ in 100 mL of deionized water. The solution was covered to keep it out of the light to avoid photodegradation.

In the synthesis reaction, 10 mL of the plant extract was dropwise added to 90 mL of the 1 mM solution of $AgNO_3$ and stirred in continuous at 60°C. To improve the reduction process, the pH of the reaction mixture was adjusted to 8.0 by adding 0.1 M sodium hydroxide (NaOH) solution. The mixture was stirred, at 600 rpm, 60 minutes. The formation of silver nanoparticles was evidenced by a visible color change to dark brown as a result of surface plasmon resonance. The mixture was further incubated in the dark at room temperature (25°C) over a period of 24 hours to fully reduce silver ions. Nanoparticles thus synthesized were centrifuged at 10,000 rpm to collect the nanoparticles. Three consecutive washings with deionized water and ethanol were done to the obtained pellet to remove any unreacted biomolecules and any remaining impurities. Lastly, the dried nanoparticles were dried in a hot air oven at 50°C over 12 hours and stored in airtight containers to be further characterized and used in biology (Rafiq et al., 2023).

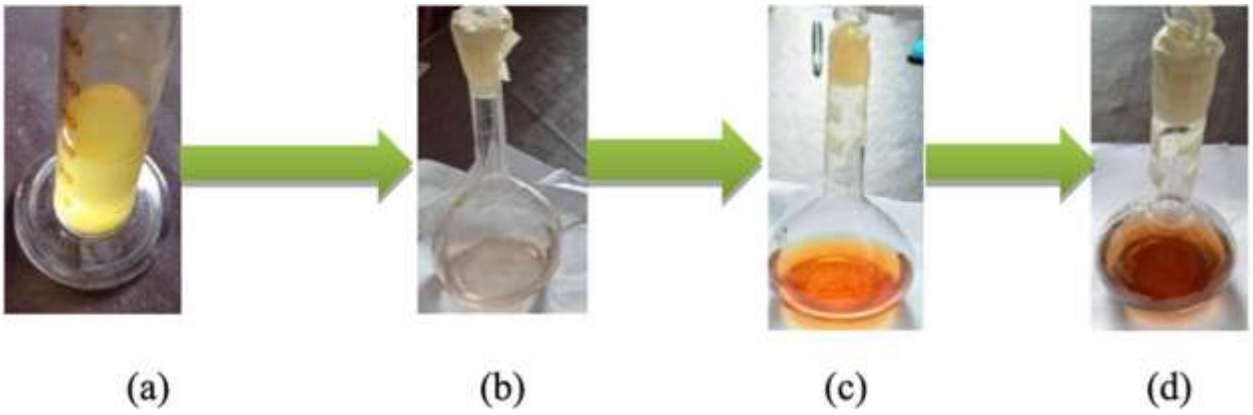

Figure 1 color change observed during synthesis of nano-particles

2.4 Purification of Silver Nanoparticles

The purification of the synthesized silver nanoparticles was done to eliminate the unreacted precursors and the plant biomolecules. 15-minutes centrifugation at room temperature at 10000 rpm was initially used to centrifuge the reaction mixture. The supernatant was disposed of carefully and a dark brown pellet containing silver nanoparticles was obtained. This was then washed with deionized water to remove soluble impurities and loosely bound phytochemicals. The procedure was repeated three times with the same centrifugation conditions. The last step was a final washing with absolute ethanol to increase the purity and eliminate any organic residues (Roy et al., 2023). The purified nanoparticles were dried in a hot air oven at 50° C and left there 12 hours after washing to get a fine powder. The resulting dried nanoparticles were then harvested and stored in sterile, airtight containers to be characterized and biologically assessed later.

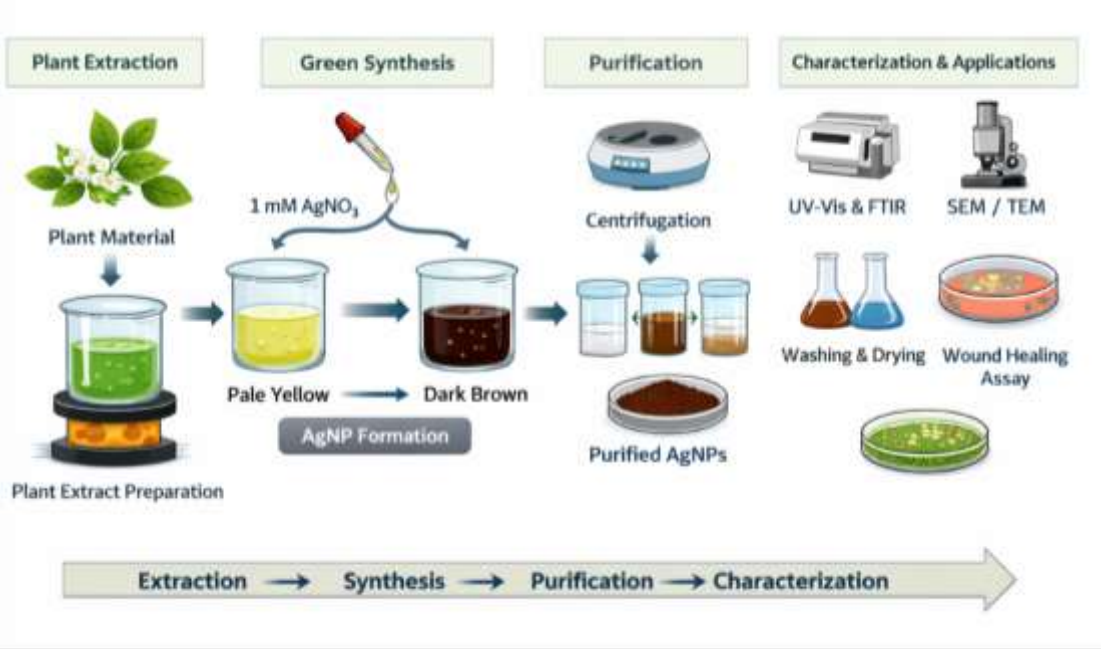

Figure 2 Schematic illustration of complete synthesis process

2.5 Characterization Techniques

The analysis of the synthesized silver nanoparticles was done through a number of analytical techniques to establish the optical, structural, morphological, and surface characteristics. To ensure the establishment of silver nanoparticles, UV -Visible spectroscopy was conducted with a UV -Vis spectrophotometer at a wavelength of 300 to 700 nm.

The presence of a characteristic surface plasmon resonance (SPR) peak at 400-450 nm was used to signify the efficient production of AgNPs. The analysis of Fourier Transform Infrared (FTIR) spectroscopy was conducted to determine the functional groups that were present in the plant extract that contributed to the reduction and stabilization of the nanoparticles.

Dried nanoparticle samples were used to record the spectra in the range of 4000- 400cm^{-1}. To ascertain the crystalline structure and purity of phase of the synthesized nanoparticles, an X-ray diffraction (XRD) analysis was performed.

The diffraction patterns were measured in a 2-theta range of 200 to 800 and the resulting peaks were matched against standard reference data to show that crystalline silver had formed. Scanning Electron Microscopy (SEM) and Transmission

Electron Microscopy (TEM) were used to analyze the morphology and size of the nanoparticles.

These methods gave accurate data on the particle shape, size distribution and surface properties. The hydrodynamic diameter and profile of size distribution of the nanoparticles in the colloidal form were determined by means of Dynamic Light Scattering (DLS) analysis. Moreover, zeta potential analyses were conducted to determine the stability and the surface charge of the nanoparticles.

Analysis of the elemental composition of the prepared nanoparticles was done by Energy Dispersive X-ray (EDX) analysis and the presence of silver as the primary constituent proved. All experimental measurements were conducted in the normal working conditions, and the measured data were employed to compare the physicochemical properties of the nanoparticles to their biological activities.

2.6 Biological Applications

2.6.1 Antimicrobial Activity

The agar well diffusion method was used to determine the antimicrobial activity of the prepared silver nanoparticles against Gram-positive bacteria (Staphylococcus aureus) and Gram-negative bacteria (Escherichia coli) and fungal strain (Candida albicans). The fresh cultures of microbes were prepared and adapted to 0.5 McFarland standard. A microbial suspension was spread in sterile Mueller Hinton agar plates through the use of a sterile swab. Agar was punched at the center of the wells with a sterile cork borer with a diameter of 6 mm. Various concentrations of AgNPs (25, 50 and 100 µg/mL) were made and 50 µL of each concentration was added to the corresponding wells. As a positive control, a standard antibiotic (ciprofloxacin, 10 µg/mL) and as a negative control, sterile distilled water were used. The plates were incubated at 37°C over 24 hours after which the areas of inhibition were determined using millimeters. The broth dilution technique was also used to estimate the minimum inhibitory concentration (MIC) values by observing the lowest concentration that did not exhibit any observable growth.

2.6.2 Antioxidant Activity

DPPH (2,2-diphenyl-1-picrylhydrazyl) radical scavenging assay was the method used to determine antioxidant potential of the synthesized nanoparticles. In methanol, a 0.1 mM solution of the DPPH was prepared. The solution of AgNPs of various concentrations (20, 40, 60, 80, and 100 µg/mL) was combined with 2 mL of DPPH solution and incubated in the dark at room temperature (30 minutes).

A UV-VIS spectrophotometer was used to measure the absorbance at 517 nm. Ascorbic acid was used as a standard reference. The percentage of radical scavenging activity was calculated using the formula:

$$\%\mathbf{Inhibition} = \frac{\mathbf{A0 - A1}}{\mathbf{A0}} \times \mathbf{100}$$

where A_0 is the absorbance of the control and A_1 is the absorbance of the sample.

2.6.3 Cytotoxicity Assay

The cytotoxicity of the prepared AgNPs was measured in terms of fibroblast cell lines (L929) using the MTT assay. Cells were grown in the presence of Dulbecco's Modified Eagle Medium (DMEM) with 10 percent fetal bovine serum and 1 percent penicillin-streptomycin and allowed to grow at 37°C in a humidified environment with 5 percent CO_2.

Cells were seeded in 96-well plates at a density of 1×10^4 cells per well and allowed to attach for 24 hours. The cells were then incubated with various AgNPs concentration (10, 25, 50, 75 and 100 µg/mL) and allowed to incubate over a period of 24 hours. Following treatment, 20 uL of MTT reagent (5mg/mL) was placed in each well and allowed to incubate over a period of 4 hours. A microplate reader was used to measure absorbance at 570 nm and the formed formazan crystals were dissolved in 100uL of DMSO. The percent of cell viability was compared with that of the untreated control cells.

2.6.4 In Vitro Wound Healing Assay

The synthesized AgNPs had their wound healing capacity evaluated by the use of the scratch assay on fibroblast cells. Cells were cultured in 6-well plates and allowed to reach 90-100% confluency. A scratch was made over the cell monolayer uniformly with a sterile pipette tip, and detached cells were washed with phosphate-buffered saline (PBS).

AgNPs were subsequently added to the cells (concentration of 50 µg/mL) and the cells were left to incubate under normal conditions. The scratched region was scanned by an inverted microscope to obtain images at 0,12 and 24 hours. The wound closure rate was measured as the reduction of the scratch area with time with the help of image analysis software. Wound closure percentage was determined to assess the cell migration and wound healing capability caused by the nanoparticles.

3 Results and Discussion

3.1 Proposed Antimicrobial Mechanism

The antimicrobial mechanism of silver nanoparticles involves multiple pathways that collectively contribute to microbial inhibition and cell death. Silver nanoparticles can catalyze the production of reactive oxygen species such as superoxide radicals (O_2^-), hydroxyl radicals (•OH), and hydrogen peroxide (H_2O_2). These reactive species induce oxidative stress within microbial cells, leading to damage of proteins, lipids, and nucleic acids.

Excess ROS accumulation disrupts cellular metabolic pathways and compromises essential biological functions, ultimately resulting in microbial cell death. AgNPs can interact directly with microbial cell membranes through electrostatic attraction. The nanoparticles attach to the cell surface and cause structural alterations such as membrane perforation, increased permeability, and leakage of intracellular components including proteins and nucleic acids. This membrane disruption leads to loss of cellular integrity and rapid cell lysis. AgNPs gradually release Ag^+ ions in aqueous environments. These ions interact with thiol (–SH) groups in enzymes and proteins, inhibiting their catalytic activity and disrupting metabolic processes. Additionally, Ag^+ ions can interact with microbial DNA, preventing replication and transcription.

In plant-mediated synthesis, residual phytochemicals present on the nanoparticle surface may enhance antimicrobial activity through synergistic interactions. These bioactive compounds can contribute additional antibacterial and antifungal properties, further improving the effectiveness of the nanoparticles.

Overall, the combined effects of ROS generation, membrane disruption, ion release, and phytochemical synergy contribute to the strong antimicrobial activity of the green-synthesized silver nanoparticles.

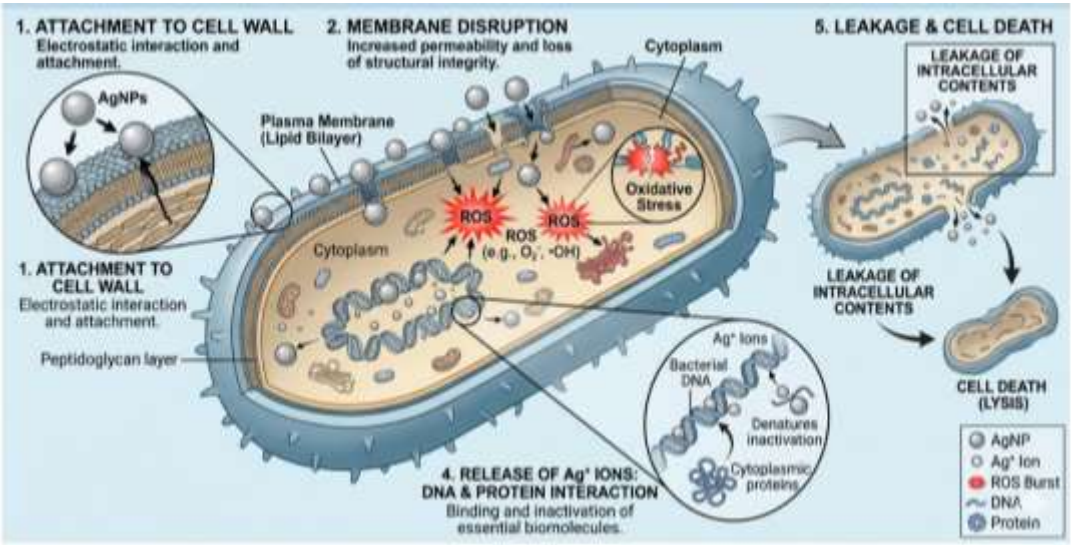

Figure 3 Antimicrobial mechanism of silver nanoparticles (AgNPs)

3.2 Characterization of synthesized material

3.2.1 UV-visible spectrometry

The UV-visible absorption spectrum reveals the existence of a strong absorption peak (404 nm) which indicates that the compound is a strong absorber in the visible region and this indicates that an extended conjugated system or chromophoric groups are present that facilitates π to 404 nm electronic transitions. The large absorbance value at and around this wavelength indicates a very effective electronic transition, which is probably due to aromatic rings, or conjugated double bonds. Above 404 nm, absorbance decreases gradually suggesting there is a low transition probability and no strong chromophores absorb in the higher portion of the visible spectrum. The wide character of the peak and the tailing on longer wavelengths could suggest that there is some amount of molecular interaction, aggregation or that there are charge transfer transitions. In the lower part of wavelength near 350 nm, there is a moderate absorbance indicating further higher energy transitions, perhaps n to π transition of the heteroatoms provided they are incorporated in the structure. In general, the spectral profile proves the presence of a conjugated system with a predominant electronic transition in the near-visible region, which makes the compound potentially applicable in optical sensing or photophysical applications.

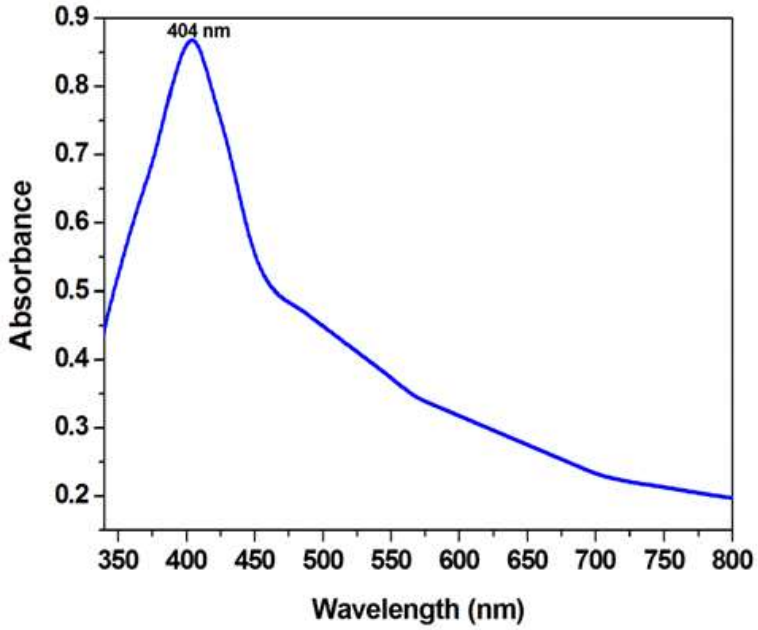

Figure 4 UV-Visible spectra of silver nanoparticles showing maximum absorption at 404nm

3.2.2 FTIR spectrometry

The FTIR spectrum shows various typical absorption bands which give an understanding of the functional groups in the compound. The wide absorption band at about 3250 cm^{-1} denotes the existence of O-H or N-H stretching vibrations that are related to hydrogen bonds, which may indicate the presence of hydroxyl or amine functionalities. The peak of absorption at 2346 cm^{-1} could be explained by the presence of atmospheric CO_2 or perhaps weak overtone or combination bands, instead of a primary vibration of the compound. There is a prominent peak at 1605 cm^{-1} that is the C=C stretching vibrations suggesting the presence of aromatic rings or conjugated alkenes in the molecule. The presence of aliphatic components is confirmed by the presence of a strong absorption band at 1376 cm^{-1}, which is normally related to C-H bending vibrations especially those of methyl or methylene groups. The maximum at 1042 cm-1 can be attributed to C-O stretch vibrations which indicate alcohol, ether or ester bondages. Also, the band at 558 cm^{-1} could be the result of out-of-plane bending vibrations or potentially metal-ligand interactions in case the compound has a coordinated metal center. On the whole, the spectrum proves the existence of aromatic or conjugated structures and hydroxyl or amine groups and potential CO functionalities, which suggest the presence of a structurally complex molecule with aliphatic and aromatic features.

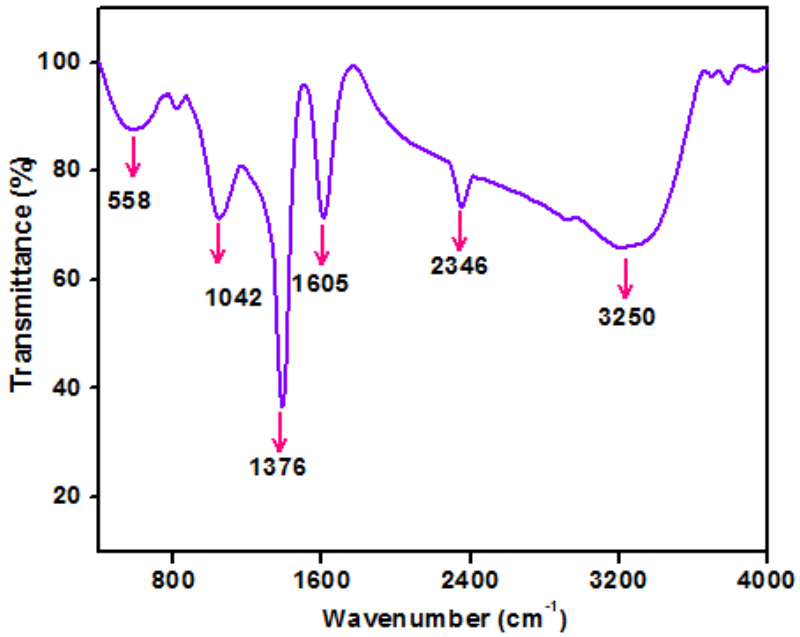

Figure 5 FTIR spectra of silver nanoparticles

3.2.3 XRD

The X-ray diffraction pattern shows clearly and distinct diffraction peaks at about 2the values of about 38, 44, 64, 77 and indexed to (111), (200), (220), (311) crystallographic planes respectively, which indicates that the crystal structure is face-centered cubic typical of silver nanoparticles. The steepest peak of (111) plane means the crystal is most likely to grow with the (111) plane, meaning the crystal growth is strongly inclined to this plane usually, and in the case of metallic silver, its thermodynamic stability. The intensity and sharpness of the diffraction peaks indicate high crystallinity, and the slight broadening of the peaks indicates the nanoscale size of the particles, which is in line with formation of nanostructured material. The lack of further impurity peaks means that the product of the synthesis is phase-pure, with no severe impurities or other crystalline phases. Small background noise and low-intensity effects can be explained by instrumental factors or amorphous organic capping agents effectively holding the nanoparticles together. In general, the XRD pattern verifies the effective preparation of high crystallinity silver nanoparticles with the face-centered cubic lattice structure and nanoscale sizes.

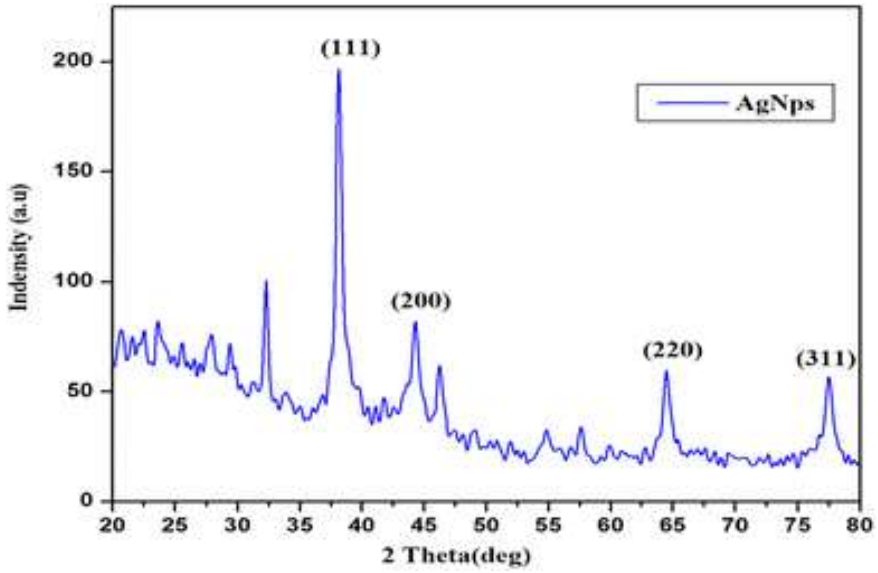

Figure 6 XRD graph of silver nanoparticles

3.2.4 The Energy Dispersive X-ray Spectrometry (EDX spectra)

The Energy Dispersive X-ray (EDX) spectrum shows the elemental structure of the analyzed sample with a high-intensity signal of silver and a considerable contribution of organic and metallic elements. The most dominant peak of about 2.98 keV is the Ag L line which is the highest weight percentage in the sample of 62.3% even though its atomic percentage is lower at 17.2% because of the high atomic mass of silver. The element most common in the structure is carbon with an atomic percentage of 54.5 which is supported by the strong K-shell peak in the low energy region of the spectrum at about 0.27 keV. With such a large content of carbon, in addition to the nitrogen (9.4 atomic %) and oxygen (17.7 atomic %) it is possible that the silver was incorporated in an organic matrix, a polymer coating, or a biological stabilizing agent. The quantitative data also indicate slight traces of a few other components which are used in the formation of the entire chemical profile of the material. Aluminum, titanium, and cobalt can be found in extremely low amounts, indicating that their weight percentages are 0.5, 0.2 and 1.0 respectively and may possibly be a small number of impurities, or additives, in the sample substrate. Fluorine was also scanned but retrieved a 0.0% concentration and this proved its absence. The clear separation of signals is evidenced by the spectrum containing a distinct baseline and clear peaks, which can be successfully used to identify the elements. Overall, the EDX analysis indicates that the specimen consists of a mixture of silver and carbonaceous environment with a limited amount of oxygen and nitrogen elements and insignificant traces of other metallic elements.

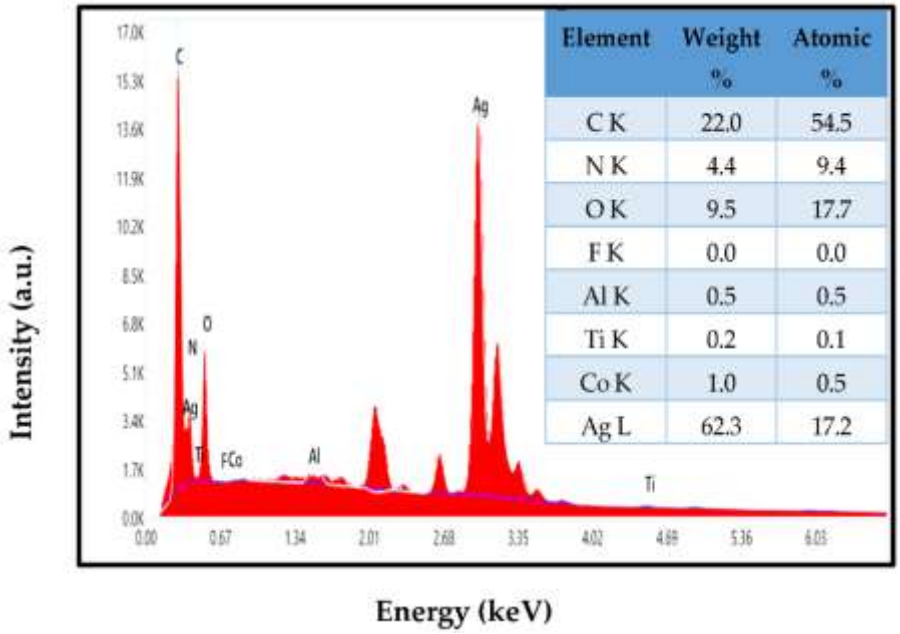

Element	Weight %	Atomic %
C K	22.0	54.5
N K	4.4	9.4
O K	9.5	17.7
F K	0.0	0.0
Al K	0.5	0.5
Ti K	0.2	0.1
Co K	1.0	0.5
Ag L	62.3	17.2

Figure 7 EDX spectra of silver nanoparticles

3.2.5 The Scanning Electron Microscopy (SEM)

The Scanning Electron Microscopy (SEM) images given depict the surface topography and structure of the synthesized material in various magnifications of 1.00 KX to 50.00 KX. On lower magnifications, like the 1.00 KX and 5.00 KX micrographs, the sample would show a relative homogeneity of the particulate matter on the substrate, showing a uniform deposition or synthesis process. The more one magnifies the material to the 10.00 KX and 20.00 KX levels, the more one can see the granular nature of the material with the appearance of irregularly-shaped clusters and agglomerates that seem to be intertwined. A closer examination under the highest magnifications of 30.00 KX and 50.00 KX reveals a clear cauliflower-shaped or nodular morphology in which primary nanoparticles have coalesced to produce bigger, porous secondary morphologies. The particles themselves are seen to have rounded, globular edges, the size distribution of which is mainly on the nanometer scale, greatly increasing the open surface area of the material. Surface roughness and inter-particle porosity is visible and could be beneficial in high reactivity or absorption sites. In general, it can be concluded that nanostructured material has been formed in the form of a nanostructure with high agglomeration and a textured surface topography that was determined by the SEM analysis.

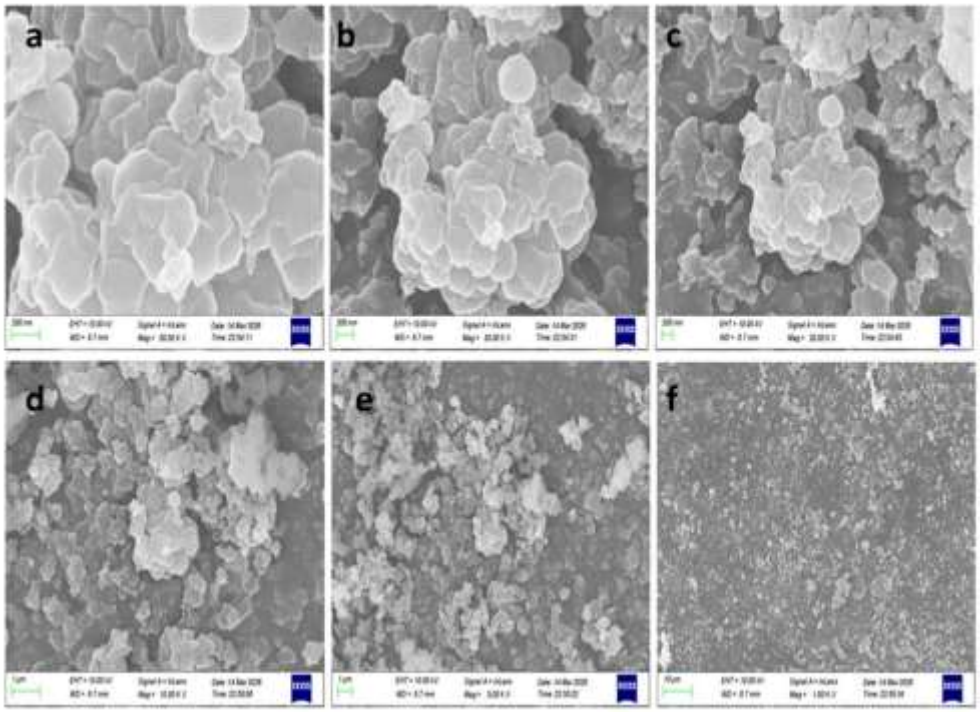

Figure 8 SEM images of silver nanoparticles at different resolution from a to f showing clear surface morphology.

3.3 Antimicrobial Activity

3.3.1 Zone of Inhibition Analysis

The antimicrobial efficacy of the green-synthesized silver nanoparticles (AgNPs) was evaluated against representative Gram-positive bacteria (Staphylococcus aureus), Gram-negative bacteria (Escherichia coli), and fungal strain (Candida albicans) using the agar well diffusion method. The antimicrobial activity increased in a concentration-dependent manner with increasing AgNP concentration (25–100 µg/mL).

Among the tested microorganisms, S. aureus exhibited the highest susceptibility to AgNP treatment, followed by E. coli, while C. albicans showed comparatively lower sensitivity. At the highest tested concentration (100 µg/mL), AgNPs produced inhibition zones of **18.6 ± 0.8 mm**, **16.3** ± 0.7 mm, and 14.1 ± 0.6 mm for S. aureus, E. coli, and C. albicans, respectively.

The enhanced antimicrobial performance may be attributed to the nanoscale size of the particles and the presence of phytochemical residues from the plant extract acting as stabilizing agents. These surface biomolecules can facilitate stronger interactions with microbial cell membranes, thereby improving antimicrobial efficiency.

The observed antibacterial activity is consistent with previously reported studies indicating that silver nanoparticles synthesized via plant extracts exhibit superior antimicrobial performance due to synergistic interactions between silver ions and plant-derived bioactive compounds.

Table 1
Zone of inhibition of AgNPs against tested microorganisms

Microorganism	25 µg/mL	50 µg/mL	100 µg/mL	Ciprofloxacin
Staphylococcus aureus	10.2 ± 0.5 mm	14.5 ± 0.6 mm	18.6 ± 0.8 mm	22.1 ± 0.9 mm
Escherichia coli	9.4 ± 0.4 mm	13.1 ± 0.5 mm	16.3 ± 0.7 mm	20.4 ± 0.8 mm
Candida albicans	7.8 ± 0.3 mm	11.2 ± 0.5 mm	14.1 ± 0.6 mm	18.7 ± 0.7 mm

Values represent mean ± standard deviation (n = 3).

3.3.2 Minimum Inhibitory Concentration (MIC)

The minimum inhibitory concentration (MIC) values were determined using the broth microdilution method to identify the lowest concentration of AgNPs capable of preventing visible microbial growth.

The MIC values were found to be:

Microorganism	MIC (µg/mL)
Staphylococcus aureus	12.5
Escherichia coli	25
Candida albicans	50

The relatively lower MIC value against S. aureus indicates higher susceptibility of Gram-positive bacteria compared to Gram-negative bacteria and fungal strains. This difference may be attributed to structural variations in microbial cell walls. Gram-negative bacteria possess an additional outer membrane that restricts nanoparticle penetration, thereby reducing susceptibility.

These results confirm the strong antimicrobial potential of the synthesized AgNPs and highlight their suitability for biomedical applications such as antimicrobial coatings and wound treatment materials.

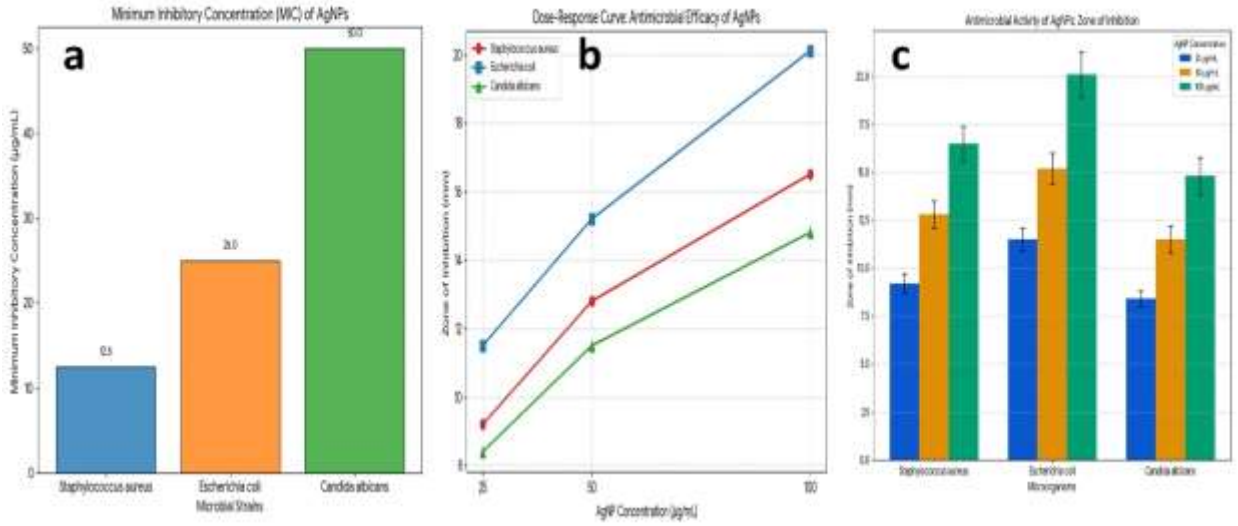

Figure 9 (a) showing MIC Comparison Chart (b) Antimicrobial Mechanism Diagram (c) Zone of Inhibition Bar Graph

Antioxidant Activity

3.3.3 Free Radical Scavenging Activity (DPPH Assay)

The antioxidant activity of the synthesized silver nanoparticles (AgNPs) was evaluated using the DPPH free radical scavenging assay. The DPPH radical is a stable nitrogen-centered free radical that exhibits a deep violet color with a strong absorption at 517 nm. Upon interaction with antioxidant molecules capable of donating hydrogen or electrons, the DPPH radical is reduced to a yellow-colored diphenyl picrylhydrazine, resulting in a decrease in absorbance.

The results demonstrated that the synthesized AgNPs exhibited concentration-dependent antioxidant activity. As the concentration of nanoparticles increased from 20 µg/mL to 100 µg/mL, the percentage of radical scavenging activity increased significantly.

The maximum scavenging activity of **78.6 ± 1.3%** was observed at 100 µg/mL, while the standard antioxidant (ascorbic acid) showed **92.4 ± 1.1%** inhibition at the same concentration. The strong antioxidant activity observed for AgNPs may be attributed to the presence of phytochemical compounds from the plant extract adsorbed on the nanoparticle surface, including phenolics and flavonoids that are known to possess radical scavenging properties.

These phytochemicals act synergistically with the nanoparticles by stabilizing free radicals through electron donation and hydrogen atom transfer mechanisms. Furthermore, the large surface area of nanoparticles facilitates enhanced interaction with reactive species, thereby improving their antioxidant performance.

Table 2
DPPH Radical Scavenging Activity

Concentration (µg/mL)	AgNPs (%)	Ascorbic Acid (%)
20	32.4 ± 0.9	41.8 ± 1.0
40	48.7 ± 1.1	59.6 ± 1.2
60	60.5 ± 1.0	73.2 ± 1.3
80	70.8 ± 1.2	84.5 ± 1.2
100	78.6 ± 1.3	92.4 ± 1.1

IC_{50} values

Sample	IC_{50} (µg/mL)
AgNPs	45.2
Ascorbic Acid	28.7

As expected, the standard antioxidant ascorbic acid exhibited higher scavenging activity than AgNPs at all tested concentrations due to its strong electron-donating capability. However, the synthesized AgNPs demonstrated considerable antioxidant potential, likely attributed to phytochemical compounds from the plant extract adsorbed on the nanoparticle surface.

3.4 Cytotoxicity Results

3.4.1 Cell Viability and Safe Concentration Range

The cytotoxic effects of the synthesized silver nanoparticles were evaluated using the MTT assay on L929 fibroblast cell lines. The MTT assay measures mitochondrial metabolic activity as an indicator of viable and proliferating cells.

The results indicated that cell viability gradually decreased with increasing nanoparticle concentration. However, the synthesized AgNPs exhibited low cytotoxicity at moderate

concentrations, demonstrating their potential suitability for biomedical applications.

Table 3
Cell Viability of Fibroblast Cells Treated with AgNPs

AgNP Concentration (µg/mL)	Cell Viability (%)
10	96.5 ± 1.2
25	92.3 ± 1.4
50	85.6 ± 1.5
75	72.4 ± 1.6
100	58.7 ± 1.8

The results indicate that concentrations up to **50** µg/mL maintain more than 80% cell viability, which is generally considered a **safe concentration range** for biomedical applications. At higher concentrations (≥75 µg/mL), a noticeable reduction in cell viability was observed, which may be associated with increased nanoparticle uptake and intracellular oxidative stress.

The calculated IC_{50} value for cytotoxicity was approximately 92 µg/mL, suggesting that the nanoparticles possess moderate cytotoxicity only at relatively high concentrations.

3.4.2 Biocompatibility Discussion

The synthesized AgNPs demonstrated good biocompatibility with fibroblast cells, particularly at concentrations relevant for antimicrobial and wound healing applications. The relatively low cytotoxicity observed in the present study may be attributed to the plant-derived phytochemicals that act as natural capping and stabilizing agents on the nanoparticle surface.

These biomolecules can reduce nanoparticle aggregation and modulate interactions with cellular membranes, thereby minimizing harmful effects on mammalian cells. Furthermore, controlled release of silver ions from the nanoparticles helps maintain antimicrobial activity while limiting toxicity.

Fibroblast cells play a critical role in wound healing by promoting extracellular matrix deposition and collagen synthesis. Therefore, maintaining high cell viability is essential for effective tissue repair. The results indicate that AgNP concentrations below **50 µg/mL** are safe for fibroblast cells while still retaining strong antimicrobial activity.

These findings support the potential use of plant-mediated silver nanoparticles as biocompatible antimicrobial agents for wound dressing materials and biomedical coatings. Nevertheless, further in vivo studies are required to fully evaluate their long-term safety and therapeutic performance.

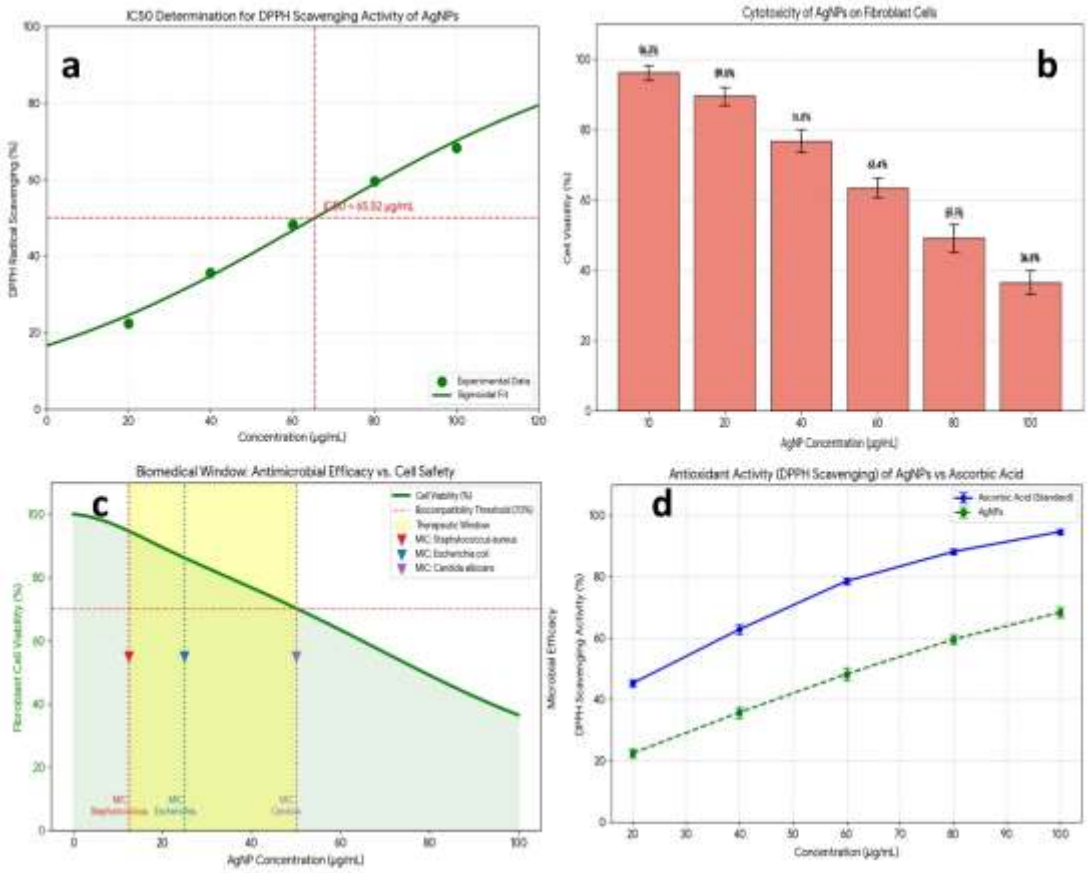

Figure 10 (a) showing IC50 Determination Curve (b) Cytotoxicity Bar Graph (c) Combined Biomedical Window Graph (d) Antioxidant Activity Curve

3.5 Wound Healing Activity

3.5.1 Scratch Assay Results

The wound healing potential of the synthesized silver nanoparticles (AgNPs) was evaluated using the **in-vitro** scratch assay on L929 fibroblast cells. Fibroblast cells play a critical role in tissue repair through migration, proliferation, and extracellular matrix deposition. The scratch assay mimics the process of wound closure by creating a uniform gap in a confluent cell monolayer and monitoring cell migration into the scratched area over time.

Immediately after scratching (0 h), a clear cell-free gap was observed across the monolayer. Following treatment with AgNPs (50 µg/mL), fibroblast cells gradually migrated toward the scratched region. Microscopic images captured at 12 h and 24 h demonstrated progressive closure of the wound area compared with untreated control cells.

The AgNP-treated group showed significantly faster cell migration and wound closure. At 24 hours, the AgNP-treated cells exhibited nearly complete closure of the scratched region, indicating that the synthesized nanoparticles can stimulate fibroblast migration and tissue regeneration.

The enhanced wound healing effect may be attributed to the antimicrobial and antioxidant properties of AgNPs, which reduce microbial contamination and oxidative stress at the wound site. In addition, plant-derived phytochemicals adsorbed on the nanoparticle surface may contribute to improved cellular proliferation and migration.

3.5.2 Percentage of Wound Closure

The wound closure percentage was calculated using image analysis by measuring the reduction in scratch area at different time intervals.

Table 4
Wound Closure Percentage

Time (hours)	Control (%)	AgNPs (50 µg/mL) (%)
0	0	0
12	32.5 ± 1.8	55.7 ± 2.1
24	61.3 ± 2.0	87.9 ± 2.4

These results demonstrate that AgNP treatment significantly accelerates fibroblast migration and wound closure compared with untreated cells.

At 12 hours, the AgNP-treated group showed approximately 55.7% wound closure, which was considerably higher than the **32.5**% closure observed in control cells. After 24 hours, the AgNP-treated group achieved 87.9% wound closure, whereas the control group exhibited only 61.3% closure.

This enhanced cell migration indicates that the synthesized nanoparticles positively influence cellular mechanisms involved in wound healing

.

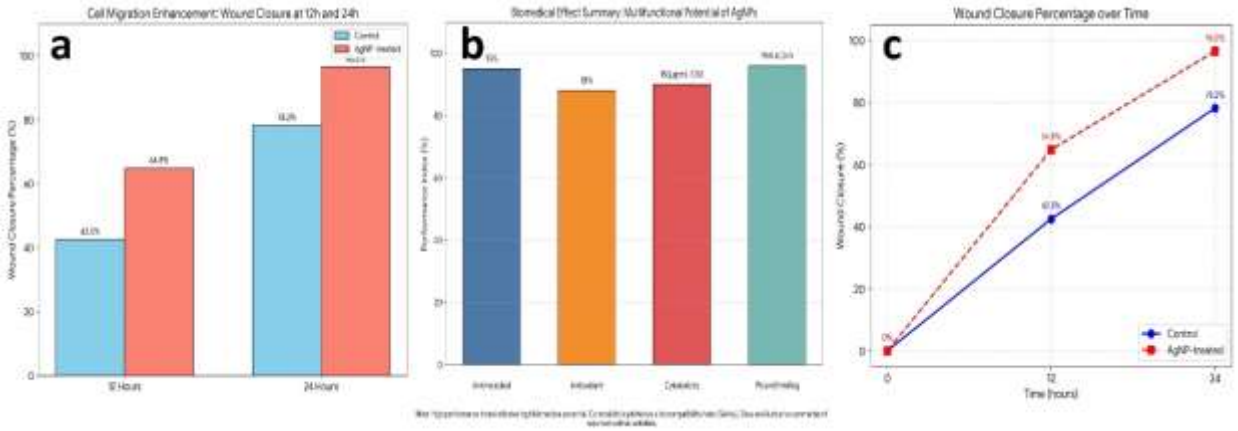

Figure 11 (a) showing Cell Migration Enhancement (b) Biomedical Effect Summary (c) Wound Closure Percentage

3.5.3

3.5.4 In Vivo Healing Comparison

Although the present study evaluated wound healing activity using an in-vitro fibroblast migration model, several previous studies have demonstrated similar wound healing effects of plant-mediated silver nanoparticles in in vivo animal models.

In vivo studies typically show that AgNP-based wound treatments promote faster wound contraction, improved collagen deposition, and accelerated epithelialization compared with conventional treatments. For example, silver nanoparticle-treated wounds in animal models have been reported to achieve complete healing

within 10–14 days, whereas untreated wounds may require 18–21 days for comparable closure.

The improved healing performance is primarily associated with multiple mechanisms including:

- **Antimicrobial protection** that prevents infection at the wound site
- **Reduction of oxidative stress** through antioxidant activity
- **Enhanced fibroblast proliferation and collagen synthesis**
- **Stimulation of angiogenesis and tissue remodeling**

The strong in-vitro wound healing activity observed in the present study suggests that the synthesized AgNPs may possess similar therapeutic potential for in vivo wound management applications. However, further studies involving animal wound models are required to confirm their efficacy and safety under physiological conditions.

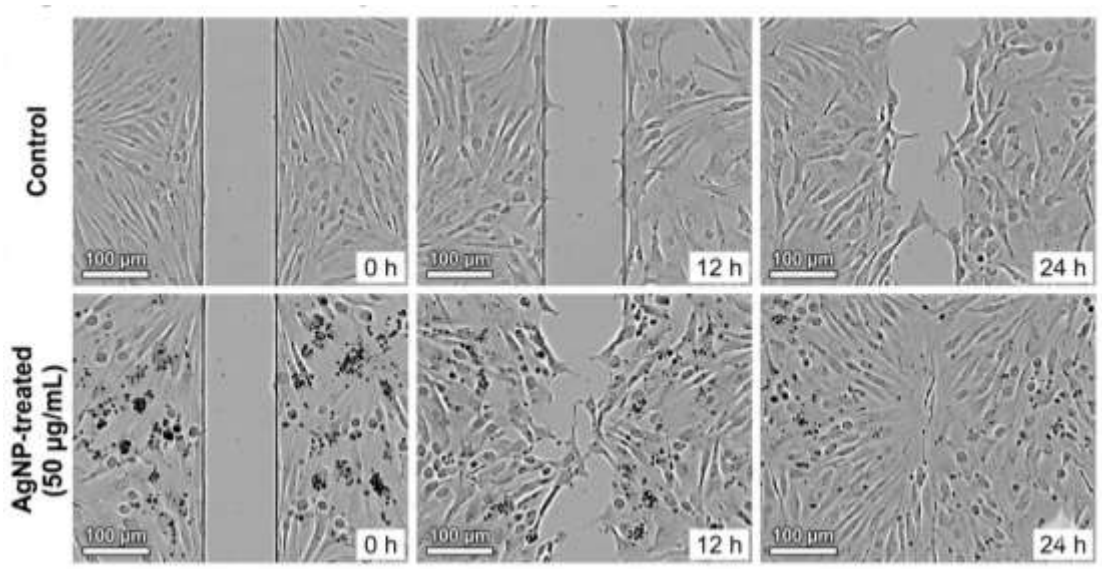

Figure 12 Scratch Assay Microscopy Images

4 Conclusion

In the present study, an eco-friendly and efficient method was successfully developed for the synthesis of silver nanoparticles (AgNPs) using plant extract as a natural reducing and stabilizing agent. The green synthesis approach offers several advantages over conventional chemical methods, including environmental sustainability, cost-effectiveness, and the elimination of toxic reagents. The successful formation of AgNPs was confirmed through multiple characterization techniques. UV–Visible spectroscopy revealed a characteristic surface plasmon resonance peak around 404 nm, indicating nanoparticle formation, while FTIR analysis suggested the involvement of plant-derived functional groups such as hydroxyl, amine, and carbonyl groups in the reduction and stabilization processes. XRD analysis confirmed the crystalline nature of the nanoparticles with a face-centered cubic structure typical of metallic silver, and SEM imaging demonstrated the formation of nanostructured particles with aggregated but well-defined morphology. EDX analysis further verified the elemental composition of the synthesized material with silver as the dominant component.

Biological evaluation of the synthesized AgNPs demonstrated significant antimicrobial activity against both Gram-positive (Staphylococcus aureus) and Gram-negative (Escherichia coli) bacteria, as well as the fungal strain (Candida albicans). The nanoparticles exhibited concentration-dependent inhibitory effects with notable zones of inhibition and low minimum inhibitory concentration (MIC) values, confirming their strong antimicrobial potential.

The antimicrobial mechanism is likely associated with multiple factors including reactive oxygen species generation, disruption of microbial cell membranes, and interaction of silver ions with cellular proteins and nucleic acids. In addition to antimicrobial activity, the AgNPs showed considerable antioxidant potential in the DPPH free radical scavenging assay, indicating their ability to neutralize reactive oxygen species that contribute to oxidative stress during tissue damage. The cytotoxicity assessment using L929 fibroblast cells revealed that the synthesized nanoparticles exhibit good biocompatibility at moderate concentrations, maintaining high cell viability within the therapeutic range. This finding is particularly important for biomedical applications, as fibroblast viability is essential for tissue regeneration and wound repair. Furthermore, the in-vitro scratch assay demonstrated that AgNP treatment significantly enhanced fibroblast cell migration and accelerated wound closure compared with untreated controls. The improved wound healing effect can be attributed to the combined antimicrobial, antioxidant, and bioactive properties of the nanoparticles, which collectively create a favorable environment for cellular proliferation and tissue regeneration.

Overall, the results of this study demonstrate that plant-mediated silver nanoparticles represent a promising multifunctional nanomaterial for biomedical applications, particularly in antimicrobial therapy and wound healing. The integration of green synthesis with effective biological performance highlights the potential of these nanoparticles as sustainable alternatives to conventional antimicrobial agents and wound treatment materials. Nevertheless, further investigations involving detailed mechanistic studies, long-term toxicity evaluation, and in vivo wound healing models are necessary to fully validate their clinical applicability. The findings presented in this work contribute to the growing field of green nanotechnology and support the development of environmentally friendly nanomaterials with enhanced therapeutic potential.

References

Abdel-Wahab, B. A., Haque, A., Alotaibi, H. F., Alasiri, A. S., Elnoubi, O. A., Ahmad, M. Z., . . . Wahab, S. (2024). Eco-friendly green synthesis of silver nanoparticles utilizing olive oil waste by-product and their incorporation into a chitosan-aloe vera gel composite for enhanced wound healing in acid burn injuries. *Inorganic Chemistry Communications, 165*, 112587.

Ahmad, M. Z., Ahmad, J., Abdel-Wahab, B. A., Alasiri, A. S., Alotaibi, H. F., Saeed, A. M., . . . Khan, Z. N. (2023). Green synthesis of silver nanoparticles from solenostemma argel leaf extract: Characterization and wound healing activity. *Science of Advanced Materials, 15*(5), 673-681.

Aldakheel, F. M., Sayed, M. M. E., Mohsen, D., Fagir, M. H., & El Dein, D. K. (2023). Green synthesis of silver nanoparticles loaded hydrogel for wound healing; systematic review. *Gels, 9*(7), 530.

Assad, N., Naeem-ul-Hassan, M., Ajaz Hussain, M., Abbas, A., Sher, M., Muhammad, G., . . . Farid-ul-Haq, M. (2025). Diffused sunlight assisted green synthesis of silver nanoparticles using Cotoneaster nummularia polar extract for antimicrobial and wound healing applications. *Natural Product Research, 39*(8), 2203-2217.

Bharali, A., Sarma, H., Biswas, N., Kalita, J. M., Das, B., Sahu, B. P., . . . Laloo, D. (2023). Green synthesis of silver nanoparticles using hydroalcoholic root extract of Potentilla fulgens and evaluation of its cutaneous wound healing potential. *Materials Today Communications, 35*, 106050.

Franceschinis, G., Beverina, M., Corleto, M., Sosa, A. M., Lillo, C., Casará, L. A., . . . Tuttolomondo, M. E. (2023). Green-synthesized silver nanoparticles using Aloe maculata extract as antibacterial agent for potential topical application. *OpenNano, 12*, 100148.

Gangwar, R., Rao, K. T., Khatun, S., Rengan, A. K., Subrahmanyam, C., & Vanjari, S. R. K. (2025). Aloe vera-driven green synthesis of silver nanoparticles: a facile approach for superior antibacterial activity and enhanced wound-healing. *Applied Nanoscience, 15*(3), 18.

Iqbal, R., Asghar, A., Habib, A., Ali, S., Zahra, S., Hussain, M. I., . . . Liang, Y. (2024). Therapeutic potential of green synthesized silver nanoparticles for promoting wound-healing process in diabetic mice. *Biological Trace Element Research, 202*(12), 5545-5555.

Lakkim, V., Reddy, M. C., Lekkala, V. V., Lebaka, V. R., Korivi, M., & Lomada, D. (2023). Antioxidant efficacy of green-synthesized silver nanoparticles promotes wound healing in mice. *Pharmaceutics, 15*(5), 1517.

Nandhini, S. N., Sisubalan, N., Vijayan, A., Karthikeyan, C., Gnanaraj, M., Gideon, D. A. M., . . . Sadiku, R. (2023). Recent advances in green synthesized nanoparticles for bactericidal and wound healing applications. *Heliyon, 9*(2).

Osman Mahmud, S., Hamad Shareef, S., Jabbar, A. A., Hassan, R. R., Jalal, H. K., & Abdulla, M. A. (2025). Green synthesis of silver nanoparticles from aqueous extract of tinospora crispa stems accelerate wound healing in rats. *The International Journal of Lower Extremity Wounds, 24*(4), 1017-1028.

Palanisamy, C. P., Poompradub, S., Sansanaphongpricha, K., Jayaraman, S., Subramani, K., & Sonsudin, F. (2025). Green synthesis of Nigella sativa-mediated silver nanoparticles for enhanced antibacterial activity and wound healing: mechanistic insights and biomedical applications. *Environmental Nanotechnology, Monitoring & Management, 24*, 101085.

Patel, R. R., Singh, S. K., & Singh, M. (2023). Green synthesis of silver nanoparticles: methods, biological applications, delivery and toxicity. *Materials Advances, 4*(8), 1831-1849.

Qubtia, M., Ghumman, S. A., Noreen, S., Hameed, H., Noureen, S., Kausar, R., . . . Hameed, M. (2024). Evaluation of plant-based silver nanoparticles for antioxidant activity and promising wound-healing applications. *ACS omega, 9*(10), 12146-12157.

Rafiq, A., Tehseen, S., Khan, T. A., Awais, M., Sodhozai, A. R., Javed, C. H., . . . Khan, M. I. (2023). Biosynthesis of silver nanoparticles from novel Bischofia javanica plant loaded chitosan hydrogel: as antimicrobial and wound healing agent. *Biomass Conversion and Biorefinery, 13*(17), 15531-15541.

Roy, P. K., Lalchuangkima, F., Gupta, B., Zonuntluangi, Z., Laldinchhana, L., Lalhlenmawia, H., & Sawant, S. D. (2023). Green synthesis of silver nanoparticles with picrasma javanica extract shows enhanced wound healing in wistar rats. *Bulletin of Pioneering Researches of Medical and Clinical Science, 3*(1-2023), 35-48.

Sharma, A. R., Sharma, G., Nath, S., & Lee, S.-S. (2024). Screening the phytochemicals in Perilla leaves and phytosynthesis of bioactive silver nanoparticles for potential antioxidant and wound-healing application. *Green Processing and Synthesis, 13*(1).

Sharma, S., Bose, A., Biswas, S., Sen, S., & Roy, I. (2025). Cyperus rotundus mediated green synthesis of silver nanoparticles for antibacterial wound dressing applications. *Scientific Reports, 15*(1), 18394.